Mécanique & Industries 11, 183–188 (2010)
www.mecanique-industries.org
Mécanique & Industries

DOI: 10.1051/meca/2010039

Mechanical contact analysis on the interfaces in a proton exchange membrane fuel cell

Zhiming Zhang[1], Christine Renaud[1], Zhi-Qiang Feng[1,a] and Hai-Ping Yin[2]

[1] Laboratoire LMEE, Université d'Évry, 40 rue du Pelvoux, 91020 Évry, France
[2] Université Paris-Est, UR Navier, ENPC, 6–8 Av. Blaise Pascal, 77455 Marne la Vallée, France

Received 9 July 2010, Accepted 12 July 2010

Abstract – The power density of a proton exchange membrane fuel cell (PEMFC) depends on several parameters. The contact resistance between the bipolar plate (BPP) and the gas diffusion layer (GDL) and the porosity of the GDL are two main parameters involved in the performance of the PEMFC. The purpose of this work is to develop a numerical model to describe the contact behavior (contact zone, contact force) on the interfaces between the different layers in order to propose an optimal structure for the high performance of PEM fuel cells. Numerical results can help to increase the knowledge of fuel cell's performance and to determine the optimal structure which can be used in the design of fuel cells.

Key words: PEM fuel cell / contact / clamping force / deformation

1 Introduction

Face to the decrease of fossil fuel resources with increasing pollution in the world, fuel cell technology becomes an area of rising interest. In all kinds of fuel cells, proton exchange membrane (PEM) fuel cells have attracted the most interest [1], due to its low operating temperature (70 °C–90 °C), quick start-up, high power density and nearly zero emissions. In general, a fuel cell is an energy conversion device that generates electricity through a electrochemical reduction reaction of oxygen and hydrogen, producing only water as a byproduct. The PEM fuel cell is typically a multi-layers structure (Fig. 1). The membrane exchange assembly (MEA) is inserted between two gas diffusion layers (GDL) coated with catalyst, and which is further sandwiched between two bipolar plates (BPP) to form one cell. Multiple cells are stacked together by the clamping bolts to provide sufficiently high power density and a desirable voltage. The clamping bolts provide sufficient pressure to avoid the gas and fluid leakage and to ensure normal operation of a PEM fuel cell.

In a PEM fuel cell stack, contact on the interface (Fig. 2) between the multi-layers is an essential condition to ensure the conductivity of electrons produced. The transfer of reactive gas and electron through the interface is important to the performance and the durability of PEM fuel cells. Multiple contacts exist on the interfaces such as (1): contact between MEA/GDL, (2): contact between BPP/GDL. On the interface BPP/GDL, more exactly it is the ribs of BPP who are in contact with the GDL. In the fuel cells, there exist power losses mainly due to the resistance because of the typical planar structure of fuel cells. Recent works revealed that around 59% of total power losses is related to the contact resistance on the interfaces of BPP/GDL [2]. In fact, the contact resistance depends strongly on contact behavior between the multi-layers of the PEMFC. One key factor influencing the contact behavior is the clamping force of fuel cells. A high clamping force can increase the electrical conductivity and the power density of fuel cells [3]. In recent research, Mishra et al. [4] and Wang et al. [5] predicted the interfacial contact resistance as a function of clamping force, material properties and surface geometry. Zhang et al. [6] developed a more accurate relation which shows that the contact resistance is directly related to the contact area on the interfaces. A large clamping force can be useful to increase the contact zones. However, a large force can lead to a low permeability of the GDL, which greatly affects the gas transfer inside the fuel cell [7]. Feser et al. [8] measured the permeability of the GDL as a function of compression ratio, and found that the permeability of the GDL decreases with the increase of the clamping force.

For the sake of simplicity, most works in this field assume that the porosity of the GDL is constant. However, this assumption may not reveal the importance of porosity to the performance of fuel cells. In fact, the clamping

[a] Corresponding author: feng@iup.univ-evry.fr

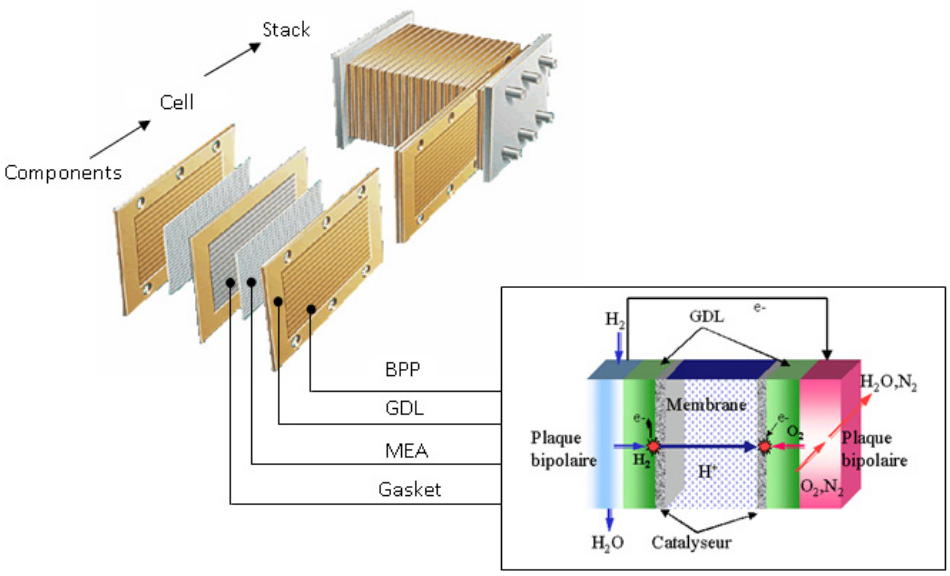

Fig. 1. Planar structure of PEM fuel cells.

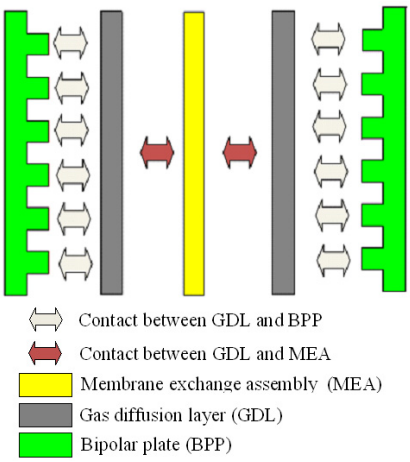

Fig. 2. Contacts at the interfaces.

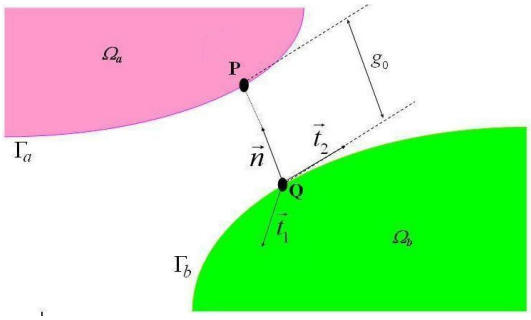

Fig. 3. Local contact frame.

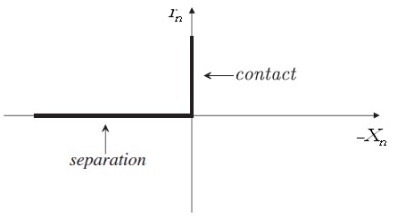

Fig. 4. Signorini conditions.

force can affect not only the interfacial contact resistance but also the porosity of the GDL in two contrary ways. A high clamping force can lead to a low contact resistance which facilitates the transfer of electrons produced, but can lead to a decrease in the porosity the GDL, which reduces the reactive gas supply. Thus, the contact zone and the deformation of the GDL on the interface should be considered together. In addition, the configuration of two objects in contact, such as the configuration of the BPP's ribs is also an important parameter influencing the mechanical contact behavior on the interfaces.

The aim of this study is to propose a numerical model to analyze the mechanical contact behavior on the interfaces. A finite-element analysis will be performed to identify the contact behavior (contact zone, contact force). An optimal clamping force can be identified in considering a low resistance and high porosity of the GDL for the more efficient fuel cells. In addition, the configuration of the BPP's ribs will be optimized.

2 Contact laws

For the sake of simplicity, only two deformable bodies Ω_α ($\alpha = a, b$), are considered (Fig. 3). The solids are elastic and undergo large deformation. Let $\boldsymbol{n}$ denote the normal unit vector at the projection point Q, directed towards Ω_a.

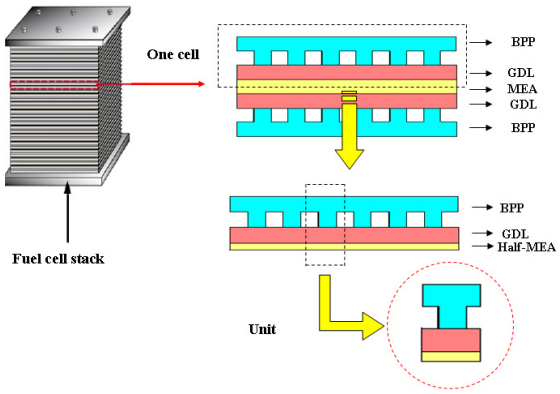

Fig. 5. Symmetric model.

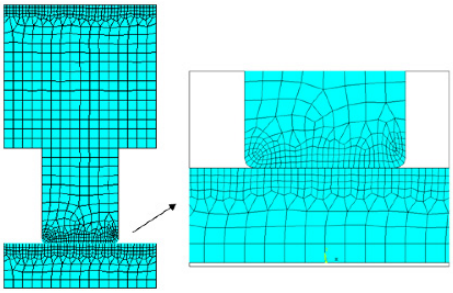

Fig. 6. Mesh.

The contact law is characterized by the Signorini conditions (Fig. 4) written in terms of the contact distance x_n, and the normal contact force r_n:

$$x_n \geq 0,\ r_n \geq 0\ ,\ r_n x_n = 0 \tag{1}$$

The Coulomb friction law is applied and represented by a Coulomb's cone:

$$K_\mu = \left\{ \boldsymbol{r} \in \mathbb{R}^3,\ \|\boldsymbol{r}_t\| \leq \mu r_n \right\} \tag{2}$$

The Signorini conditions and the Coulomb law define a complete contact law which is a complex non smooth dissipative law including three statuses: no contact, sticking contact and sliding contact. The contact problem can be solved by the boundary element method [9], the augmented Lagrangian method [10] and the analytical method [11]. In this work, the augmented Lagrangian method is used to calculate the reaction forces on the contact interfaces. The reader can refer to [10, 12] for more details on the solution method.

3 Numerical modeling

The finite element code FER/Contact developed in our laboratory is used to build the FEM model as shown in Figures 5 and 6. The chemical reaction and the fluid phenomenon are not considered in this study. Considering the geometrical repetitive parts of MEA, GDL and BPP, it is practical to choose a parametric modeling, which can not only avoid geometrical repetition work in the contact modeling, but also can easily modify the parameters to study its influence on the performance of fuel cells. The material of the fuel cells is assumed to be linear and elastic. Mechanical and geometrical properties of fuel cells are cited from reference [13].

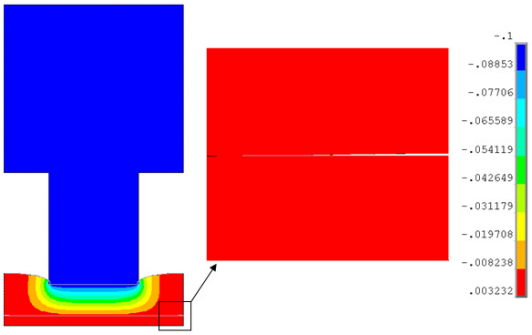

Fig. 7. Contact separation.

In the FEM modeling, a 2D 8-nodes element is used to mesh the whole model (Fig. 6). A finer mesh should be considered around the contact zones. A finer mesh should be also used at the round radius of the BPP's ribs where the major variation of contact behavior occurs. The fine size of element is 0.025 mm and the size of elements is 0.1 mm for the other areas. Thus, the entire model has 964 elements and 3122 nodes. The normal displacements at the left, right boundaries of the GDL and the bottom boundaries of the MEA were restricted due to the symmetry of the structure. The vertical displacement of the BPP's top boundary is given downwards, simulating the stacking process, which is determined by the sealing compression level in perfect condition.

4 Numerical results and analysis

4.1 Contact behavior on the interfaces

As we can see from Figure 7, the deformation of GDL is more important than that of MEA and BPP, and moreover a contact separation is observed at the extremities between MEA and GDL. But no separation happens between BPP and GDL. Figure 8 shows that the contact zone between MEA and GDL has zero contact pressure at the extremities which corresponds to the contact separation as shown in Figure 7. The separation occurred between MEA and GDL may lead to the high contact resistance and a low performance of fuel cells which should be avoid in the construction of fuel cell stack. The thermal annealing process [14] is proposed to eliminate the separation between MEA and GDL. It is realized under a certain temperature and sufficient pressure and the catalysts are used to improve the transport properties between different layers, reducing the contact resistance on the interfaces and increasing the stability and performance of fuel cells. For this reason, in the numerical modeling, the MEA and the GDL are always glued together in order

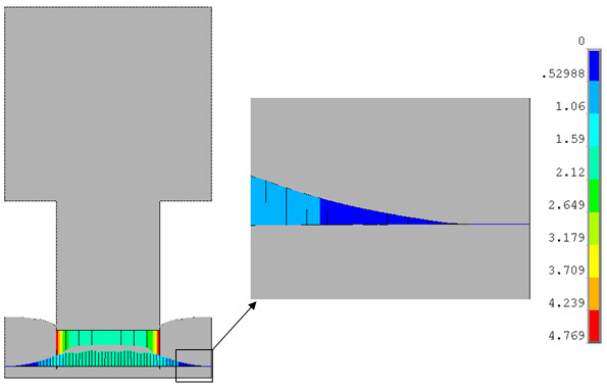

Fig. 8. Contact pressure.

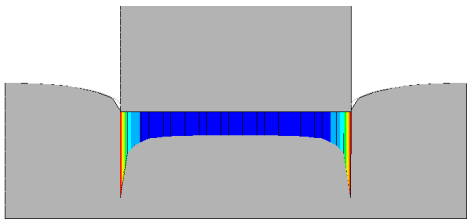

Fig. 9. Pressure with right corner rib.

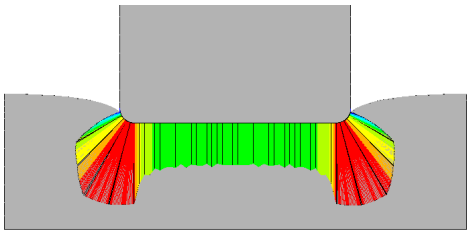

Fig. 10. Pressure with round corner rib.

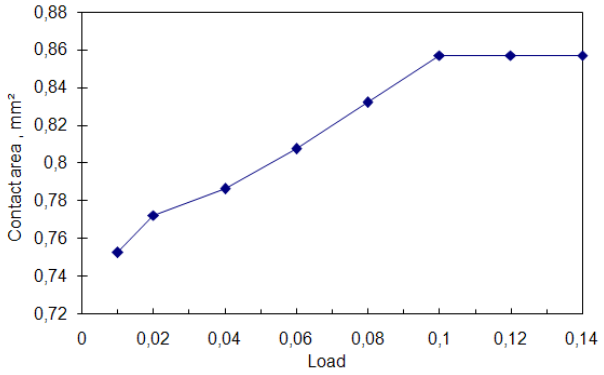

Fig. 11. Contact area vs. applied load.

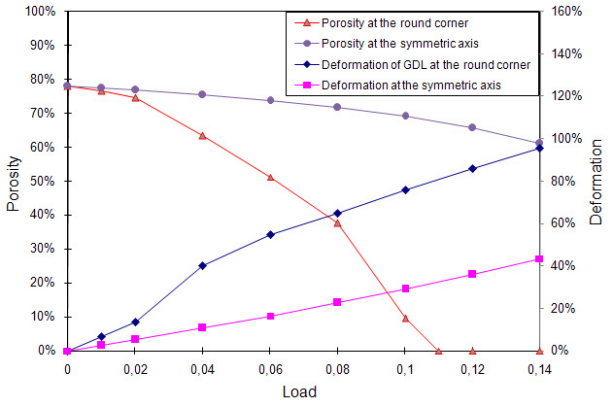

Fig. 12. Deformation, porosity vs. load.

to make sure of no separation on the interface. In the following analysis, the contact zone exists only on the interfaces between GDL and BPP. Figures 9 and 10 show the contact pressure distribution on the interfaces with a right corner rib and a round corner rib. The contact pressure is quite high if BPP has a right rib, and obviously an increase of the round radius can reduce the local concentration of pressure and improve the uniformity of pressure distribution on the interfaces.

4.2 Influence of clamping loads

Figure 11 shows that the contact area on the interfaces is effectively affected by clamping loads. When the prescribed displacement is less than 0.1 mm, the contact area increases with the load. If the displacement is more than 0.1 mm, the contact area becomes constant and equals to 0.85704 mm^2, i.e., no more contact zone will be produced even the load increases. The load can also cause the deformation of the GDL which can directly affect the porosity of the GDL. The deformation of the GDL at the round corner and at the symmetric axis on the interface is important and must be studied. As we can see from Figure 12, the deformation of GDL increases with load whereas the porosity of GDL decreases. For a displacement of about 0.11 mm, the porosity of GDL tends to zero which prevents the supply of reactive gas inside the fuel cells. Furthermore, as a byproduct of electrochemical reaction, the water is difficult to evacuate outside which will lead to a low performance of fuel cells. As the variation of the deformation at the symmetric axis is small, the porosity of GDL decreases slightly from about 78% to 60%. These studies clearly indicate that under an appropriate load, we can get a maximum contact area while keeping the best possible porosity of GDL. In our study, the load of 0.1 mm is the optimal choice.

4.3 Influence of rib's round corner radius

The contact state changes mainly at the rib's round corner during loading and is influenced by the rib's corner radius R. Figure 13 shows the distribution of contact area with R. The contact area on the interfaces increases at the beginning and then decreases. The peak value occurs when $R = 0.05$ mm which shows that for each load, there exists a suitable round corner radius corresponding to the maximum contact area on the interfaces. In Figure 13, the contact area (0.808 mm^2) with the radius

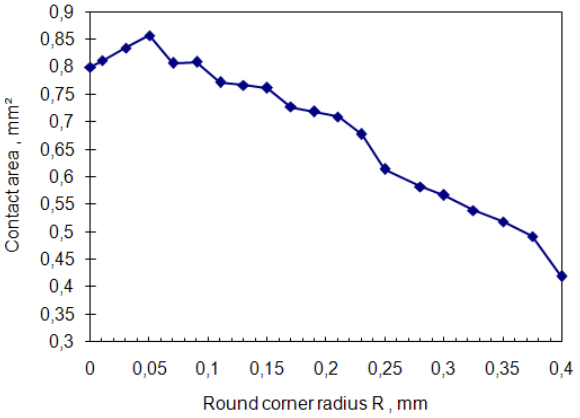

Fig. 13. Contact area vs. R.

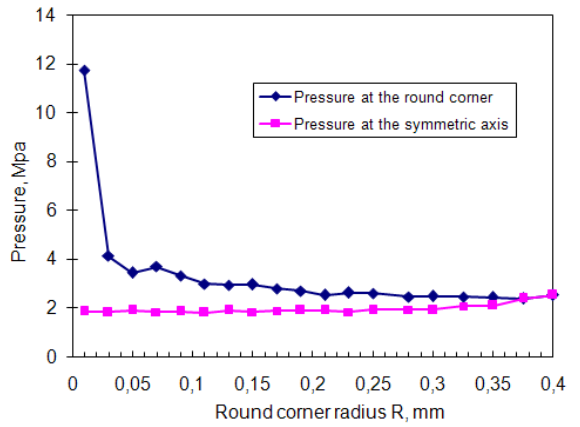

Fig. 14. Pressure vs. R.

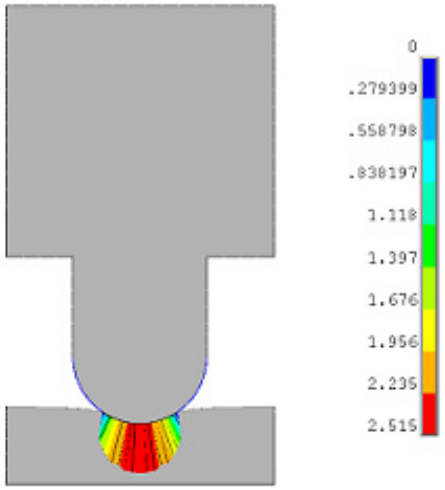

Fig. 15. Pressure ($R = 0.4$ mm).

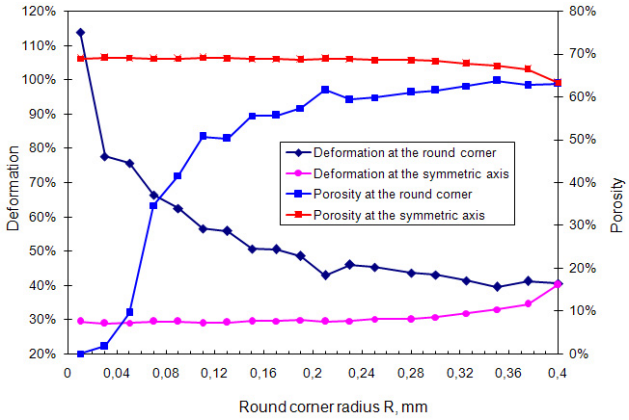

Fig. 16. Deformation and porosity vs. R.

of 0.09 mm is nearly equivalent to contact area (0.8 mm^2) with a right corner. However the contact area decreases with a more large round corner radius, the minimum contact area is at a radius of 0.4 mm, where the configuration of BPP's rib is semicircle. So we can find that for a larger contact area, a rectangle rib of BPP with a small R (from 0.01 to 0.09 mm) is better than that of rectangle rib with right corner. In addition, a reasonable round corner is also proposed to reduce the local stress concentration on the interfaces. Figure 14 shows the distribution of contact pressure at the round corner and at the symmetric axis on the interfaces. It can be observed that a round corner can obviously reduce the stress singularity of right corner. In the case of $R = 0.4$ mm, the contact pressure at the round corner on the interfaces corresponds to the contact pressure at the symmetric axis at the peak point of the semicircle rib (Fig. 15). Figure 16 shows the evolution of deformation and porosity of the GDL with respect to R. It can be observed that, globally, the deformation of the GDL decreases with R and on the other side, the porosity of the GDL increases. It is observed that a larger R can improve the porosity of GDL. When the radius varies from 0.01 mm to 0.1 mm, the porosity at the round corner increases of 42%, then the curve increases more smoothly to 63% with $R = 0.4$ mm. As a conclusion, if we consider all together the contact area, the contact pressure and the porosity of GDL, $R = 0.05$ mm is an optimal choice in our study.

5 Conclusion

In this paper, we have proposed a finite element model and a numerical application to the case of contact behavior on the interfaces between multi-layers of PEM fuel cells. From numerical experiments, we have found that:

- The unilateral contact (BPP/GDL) model with a reasonable round corner of ribs is proposed which can not only avoid the contact separation between the interface of MEA and GDL, but also can improve the local stress distribution on the interfaces.
- The contact area increases with the load whereas the porosity decreases. An optimal load exists to satisfy a low contact resistance and the high porosity of GDL.
- An optimum value of $R = 0.05$ mm has been determined allowing a low stress concentration, a low contact resistance and a high porosity of GDL.

As the GDL is a porous material, it would be interesting to deepen our work on the modeling of multi-porous layer in some areas where local porosity behavior is important. The work is being undertaken.

References

[1] G. Hoogers, Fuel cell Technology Handbook, CRC Press, 2002

[2] http://bama.ua.edu/~rreddy/projects/fuel_cells.htm

[3] W.R. Chang, J.J. Hwang, F.B. Weng, S.H. Chan, Effect of clamping pressure on the performance of a PEM fuel cell, J. Power Sources 166 (2007) 149–154

[4] V. Mishra, F. Yang, R. Pitchumani, Measurement and prediction of electrical contact resistance between gas diffusion layers and bipolar plate for applications to PEM fuel cells, J. Fuel Cell Sci. Technol. 1 (2004) 2–9

[5] H.L. Wang, M.A. Sweikart, J.A. Turner, Stainless steel as bipolar plate material for PEMFCs, J. Power Sources 115 (2003) 243–251

[6] L.H. Zhang, Y. Liu, H.M. Song, S.X. Wang, Y.Y. Zhou, S.J. Hu, Estimation of contact resistance in proton exchange membrane fuel cells, J. Power Sources 162 (2006) 1165–1171

[7] P.M. Wilde, M. Mandle, M. Murata, N. Berg, Structural and physical properties of GDL and GDL/BPP combinations and their influence on PEMFC performance, Fuel Cells 3 (2004) 180–184

[8] J.P. Feser, A.K. Prasad, S.G. Advani, Experimental characterization of in-plane permeability of GDLs, J. Power Sources 162 (2006) 1226–1231

[9] C. Renaud, Z.-Q. Feng, BEM and FEM analysis of Signorini contact problems with friction, Comput. Mech. 31 (2003) 390–399

[10] Z.-Q. Feng, 2D or 3D frictional contact algorithms and applications in a large deformation context, Commun. Numer. Meth. Eng. 11 (1995) 409–416

[11] I.F. Kozhevnikov, D. Duhamel, H.P. Yin, Z.-Q. Feng, A new algorithm for solving the multi-indentation problem of rigid bodies of arbitrary shapes on a viscoelastic half-space, Int. J. Mech. Sci. 52 (2010) 399–409

[12] P. Joli, Z.-Q. Feng, Uzawa and Newton algorithms to solve frictional contact problems within the bi-potential framework, Int. J. Numer. Meth. Eng. 73 (2008) 317–330

[13] K. Jiao, X.G. Li, Effects of various operating and initial conditions on cold start performance of polymer electrolyte membrane fuel cells, Int. J. Hydrogen Energy 34 (2009) 8171–8184

[14] J.E. Hensleya, J.D. Waya, S.F. Decb, K.D. Abneyc, The effects of thermal annealing on commercial nafion membranes, J. Membr. Sci. 298 (2007) 190–201